

Project information

Project full title	Connecting Russian and European Measures for Large-scale Research Infrastructures – plus
Project acronym	CREMLINplus
Grant agreement no.	871072
Instrument	Research and Innovation Action (RIA)
Duration	01/02/2020 – 31/01/2024
Website	www.cremlinplus.eu

Deliverable information

Deliverable no.	D2.7
Deliverable title	Design of beam monitors, target chambers, beam pipes
Deliverable responsible	FAIR
Related Work-Package/Task	WP2
Type (e.g. Report; other)	Report
Author(s)	Senger et al.
Dissemination level	Public
Document Version	
Date	
Download page	

Document information

Version no.	Date	Author(s)	Comment
1	16.12.2020	Anna Senger, Peter Senger Adrian Rost, Tetyana Galatyuk, Jerzy Pietraszko	Beam pipe/target chamber simulations, Design of beam monitors



This project has received funding from the European Union's Horizon 2020 research and innovation programme under grant agreement No. 871072.

Table of Contents:

1. Beam pipe studies for the CBM experiment at FAIR
 - 1.1 Simulation framework and input
 - 1.2 Beam properties
 - 1.3 Beam pipe in STS and RICH/MuCh
 - 1.4 Beam pipe through TRD, TOF and PSD to beam dump
 - 1.5 Radiation background around the beam pipe
 - 1.6 Next steps
2. Beam pipe and target chamber studies for the BM@N experiment at NICA
 - 2.1 Radiation calculations without and with beam pipe
 - 2.2 Preliminary design of the BM@N target chamber and beam pipe
3. Design of beam monitors and T0 counters for the CBM experiment at FAIR
 - 3.1 Introduction
 - 3.2 Concept of diamond based T0 detector for Day-1
 - 3.3 Beam halo measurement concept
 - 3.4 Mechanical integration
 - 3.5 Read-out concept
 - 3.6 Summary and outlook

Task 2.4 Design of beam monitors, target chambers, beam pipes

1. Beam pipe studies for the CBM experiment at FAIR

1.1 Simulation framework and input

The task of the beam pipe is to guide a high-intensity beam of up to 10^9 Au ions/s from the SIS100 synchrotron at FAIR through the CBM setup to the beam dump without producing significant background radiation in the various detector stations, taking into account the broadened beam profile due to multiple scattering in the target, and the deflection of the beam in the field of the CBM dipole magnet. In a first step, detailed simulations have been performed using the codes FLUKA [1] and GEANT3 [2], in order to define the shape of the beam pipe. Gold beams with kinetic energies between 2A and 10A GeV have been used to study the interaction of the beam with the target, the detector materials, the proposed beam pipe and the beam dump. The left panel of figure 1 depicts the geometry of the CBM detector setup as implemented in CBMroot and used for physics simulations. In the right panel of figure 1 the CBM detector model is shown, which is used in the FLUKA calculations for radiation studies and the design of the beam pipe.



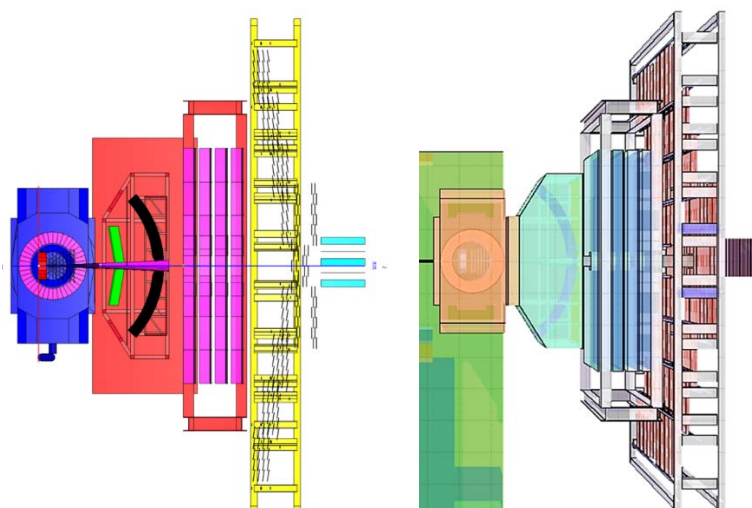


Fig. 1: Sketch of the CBM setup as implemented in CBMroot (left) and in FLUKA (right). The CBMroot version is used for physics simulations, the FLUKA version for the radiation studies presented in this note. Both versions represent the so called electron setup comprising the magnet with the Micro-Vertex Detector (MVD) and the Silicon Tracking System (STS) inside, the Ring Imaging Cherenkov (RICH) detector, the Transition Radiation Detector (TRD), the Time-of-Flight (TOF) wall, and the Projectile Spectator Detector (PSD).

1.2 Beam properties

For the design of the beam pipe and the beam dump the beam profile after the target has to be considered. The typical size of the SIS100 Au beam hitting the target is $\Delta x = \Delta y = 0.6$ mm with a divergence of 1.7 mrad (Sebastian Ratschow, private communication). The left panel of figure 2 depicts the horizontal profile of an Au beam with an energy of 2A GeV at a distance of 1.6 m after a 250 μm thick Au (1% interaction) target as calculated with FLUKA for a typical SIS100 beam (red) and for a point-like beam (blue). The comparison clearly demonstrates that the beam profile is generated by multiple scattering in the target. The right panel of figure 2 exhibits the comparison between FLUKA and GEANT3 results for the same beam, target and distance. Both codes agree in the description of multiple scattering of an Au beam in an Au target. The deflection of the beam is due to the magnetic field which was assumed to be 100% ($BL = 1$ Tm).

The deflection of a gold beam due to the magnetic field of the CBM dipole is illustrated in figure 3 for beam kinetic energies between 2A and 8A GeV and the full magnetic field integral of 1 Tm. For energies above 6A GeV the beam still hits the iron core of the beam dump, while for lower energies this is no longer the case. This situation already requires the lowering of the magnetic field for low Au beam energies. Low-energy beams with a larger Z/A ratio than Au, in particular protons, require even lower magnetic fields. The calculations show already that the position of the PSD has to be adjusted to the beam energy.



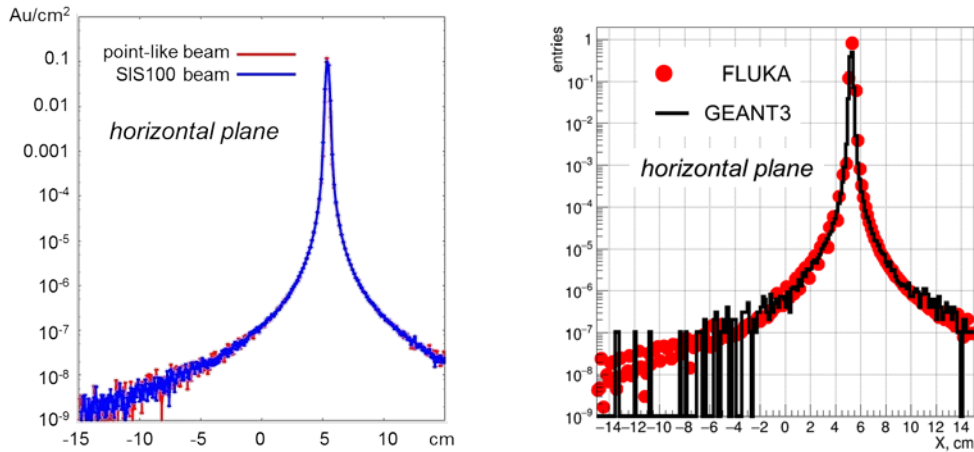


Fig. 2: Horizontal profile of an Au beam with kinetic energy 2A GeV at a distance of 1.6 m downstream a 250 μm thick Au target for full magnetic field. Left panel: FLUKA calculations assuming a typical SIS100 Au beam with $\Delta x = \Delta y = 0.6$ mm and a divergence of 1.7 mrad (blue histogram) compared to a pencil-like beam (red histogram). Right panel: FLUKA results (red dots) in comparison with GEANT3 results (black histogram). The distributions are normalized to one Au ion.

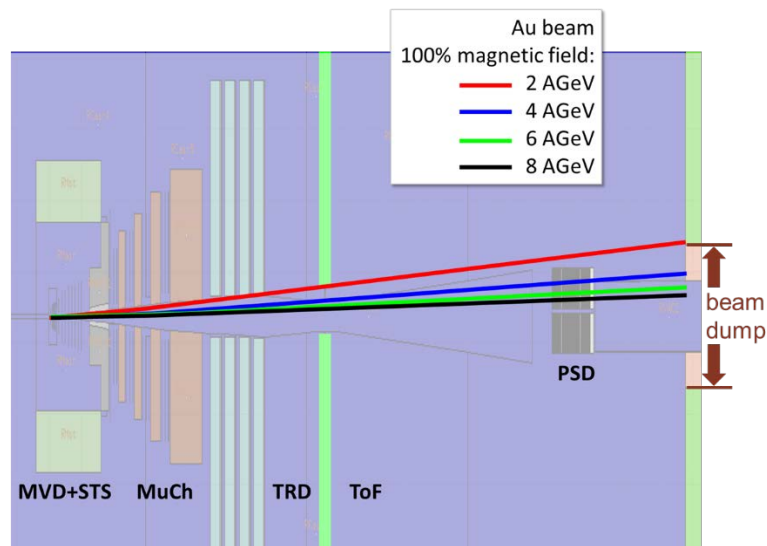


Fig.3: Deflection of Au beams with kinetic energies between 2A and 8A GeV by the magnetic field with an integral of $BL = 1$ Tm (= 100%)

Figure 4 depicts the beam profile at the entrance of the beam dump for Au beam kinetic energies between 2A and 10A GeV for scaled magnetic fields. The scaling factors for the different beam energies were taken from the Technical Design Report of the PSD. The 6A GeV beam (green line) would still be well within the iron core of the beam dump if the scaling factor of 60% would be increased to 80% or 90%.



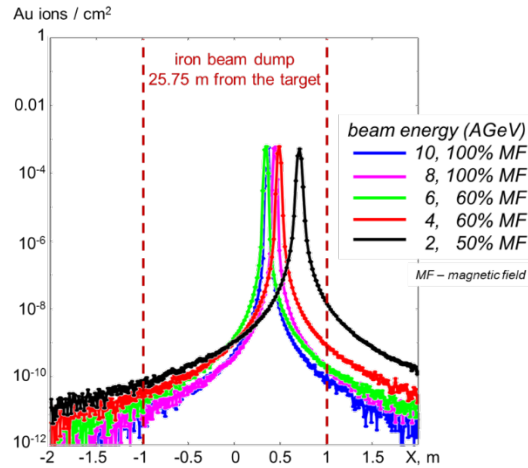


Fig.4: Horizontal profiles of Au beams with kinetic energies from 2A to 10A GeV traversing a 250 μm thick Au target at the entrance of the beam dump for different scaling factors of the magnetic field as proposed in the TDR of the PSD. The distributions are normalized to one Au ion.

1.3 Beam pipe in STS and RICH/MuCh

The beam pipe within the STS has been designed and a prototype has been built. The technical drawing is shown in figure 5 (Wolfgang Niebur, private communication). This beam pipe, which consists of carbon fiber of 0.5 mm thickness, has been used in the FLUKA calculations.

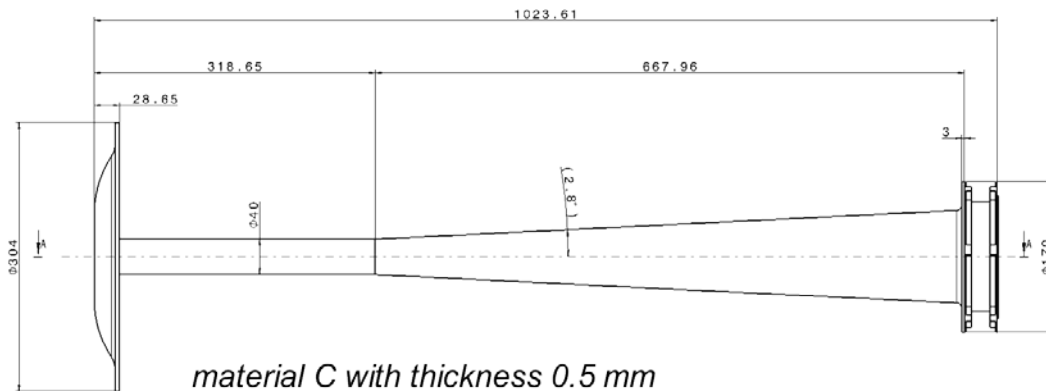


Fig. 5: Beam pipe within the STS.

The Au beam profiles for kinetic energies between 2A and 10 A GeV at a distance of 50 cm behind the 250 μm thick Au target are show in figure 6 for scaled magnetic fields. The beams are well confined within the beam pipe.



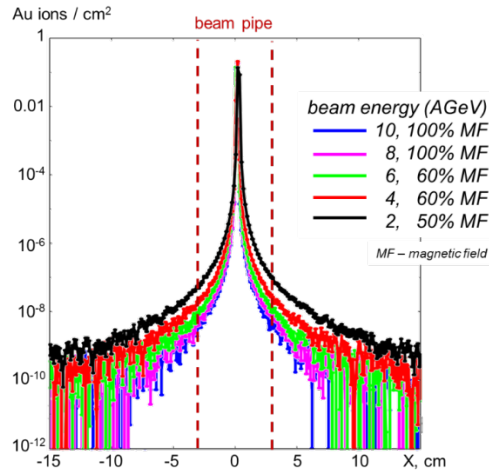


Fig.6: Au beam profiles for kinetic energies between 2A and 10 A GeV at a distance of 50 cm behind the 250 μm thick Au target for scaled magnetic fields. The distributions are normalized to one Au ion.

The STS beam pipe ends with a flange (see figure 5) and is followed by the beam pipe within the RICH or the MuCh detector. These two beam pipes have to fulfil very different requirements concerning material budget, and will be designed for each detector separately. However, these beam pipes should agree in their general shape in order to fit to the upstream STS beam pipe and to the downstream TRD and TOF beam pipe. For the following design considerations and corresponding calculations it is assumed that the RICH/MuCh beam pipe continues like the conical part of the STS beam pipe, resulting in a radius of $R = 7.47$ cm at a distance of 170 cm downstream the target, and a radius of $R = 16.16$ cm at a distance of 370 cm. The corresponding beam profiles are shown in figure 7. For the calculations it is assumed that the beam pipe consists of carbon fiber with 0.5 mm wall thickness.

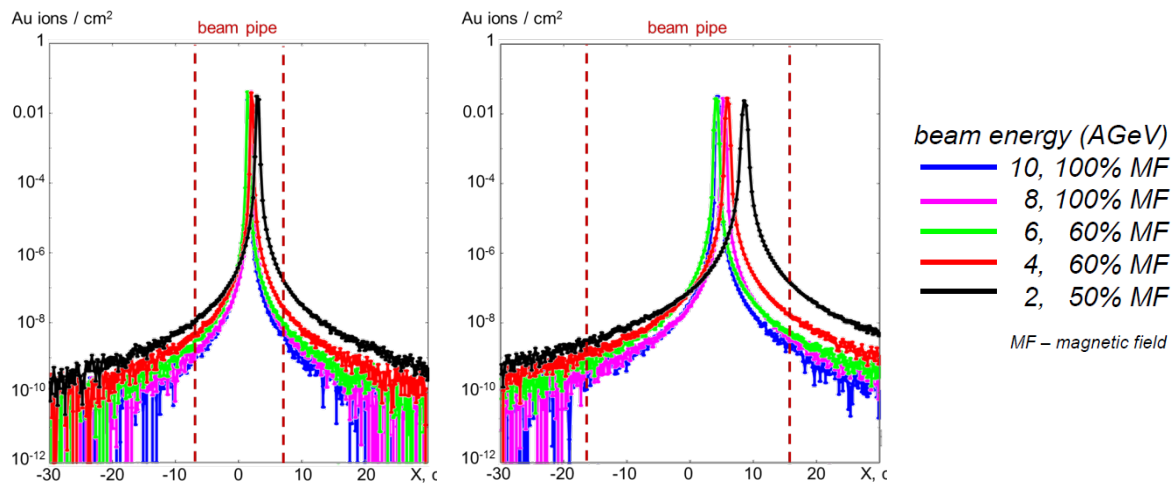


Fig. 7: Au beam profiles for kinetic energies between 2A and 10 A GeV at a distance of 170 cm (left panel) and 370 cm (right panel) behind the 250 μm thick Au target for scaled magnetic fields. The distributions are normalized to one Au ion.



1.4 Beam pipe through TRD, TOF and PSD to beam dump

It can be seen in figure 7 that at a distance of 3.7 m downstream the target the beams are displaced from the center of the beam pipe, and one tail of the beam distributions starts to hit the beam pipe. Moreover, when continuing with a conical beam pipe, it would not fit into the inner holes of TRD, TOF and PSD. Therefore, it is assumed for the following simulations that the beam pipe will continue with a cylindrical shape, which is tilted to confine the beam in the center until it reaches the beam dump. Figure 8 depicts two beam pipe options with a bellow between RICH/MuCh and the TRD detector. In the upper panel of figure 8 a cylindrical beam pipe is shown with a radius of $R = 16.16$ cm up to the entrance of the PSD, where the radius is reduced to $R = 9.5$ cm in order to fit into the hole of the PSD. The reduction of the radius is accompanied by a shift of the beam pipe in order to keep the beam in the center of the smaller pipe. The beam pipe version shown in the lower panel of figure 8 features also a bellow between RICH/MuCh and TRD, but reduces the radius to $R = 9.5$ cm and re-centers the pipe directly behind the bellow. For both beam pipe options the bellow has to provide a kink angle between 0.7 and 1.8 degrees for Au beams with energies of 10A and 2A GeV, respectively. The tilt of the beam pipe according to the magnetic rigidity of the beam requires the corresponding movement of the mechanical structures of the pipe including pumps, and of the PSD. For the following simulations it is assumed that the beam pipes consists of carbon fiber with 0.5 mm wall thickness.

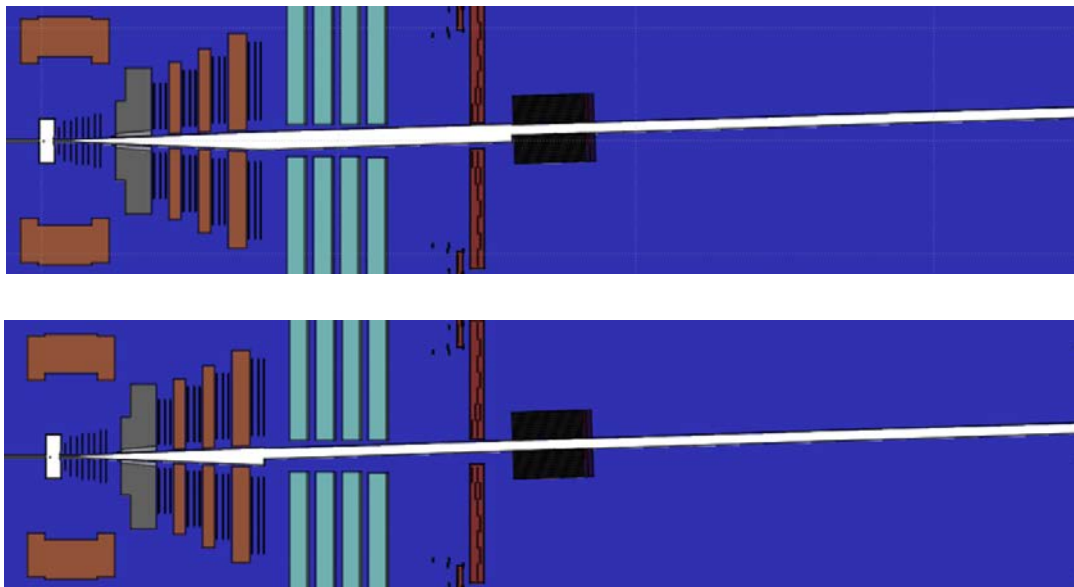


Fig.8: Two options for the beam pipe from TRD to the beam dump (see text).

The results of the FLUKA calculations in terms of charged-particle rate density in the TRD for the two beam pipe options are shown in figure 9. The simulations were performed for an Au beam with kinetic energy of 2A GeV, an intensity of 10^9 ions/s, 50% magnetic field, and a 1% interaction Au target. The dashed rectangle corresponds to the hole in the TRD detector, the black circles represent the beam pipe with a radius of $R = 9.5$ cm (left panel) and $R = 16.16$ cm (right panel).



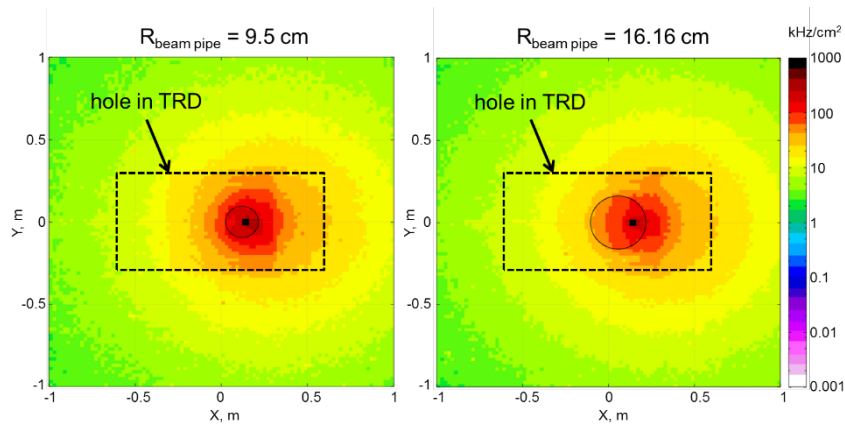


Fig.9: Charged-particle rate densities in the TRD for the beam pipe with radius $R = 9.5 \text{ cm}$ (left) and $R = 16.16 \text{ cm}$ (right) (see text).

The charged-particle rate densities in the TOF detector for the two beam pipe options are shown in figure 10. The simulations were also performed for an Au beam with kinetic energy of 2A GeV, an intensity of 10^9 ions/s, 50% magnetic field, and a 1% interaction Au target. In this case the Beam Fragmentation T0 Counter (BFTC) was located close to TOF wall, and had to be shifted according to the kink angle of the beam pipe.

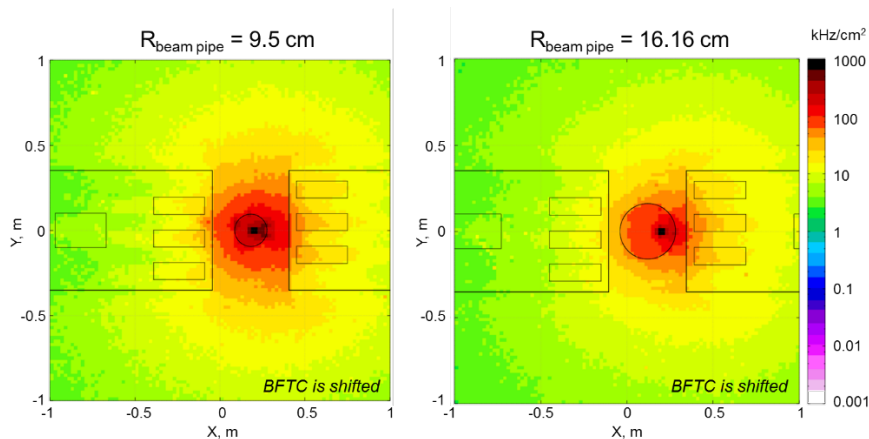


Fig.10: Charged-particle rate densities in the TOF for the beam pipe with radius $R = 9.5 \text{ cm}$ (left) and $R = 16.16 \text{ cm}$ (right) (see text).

1.5 Radiation background around the beam pipe

The ionizing and non-ionizing doses around the beam pipe have been calculated with FLUKA for an Au beam with kinetic energy of 2A GeV, an intensity of 10^9 ions/s over 2 months, 50% magnetic field, and a 1% interaction Au target. In figure 12 the ionizing dose is shown for the two beam pipe options in the horizontal plane through the beam pipe. The results do not differ significantly for the two options. The same is true for the non-ionizing dose which is shown in figure 13.



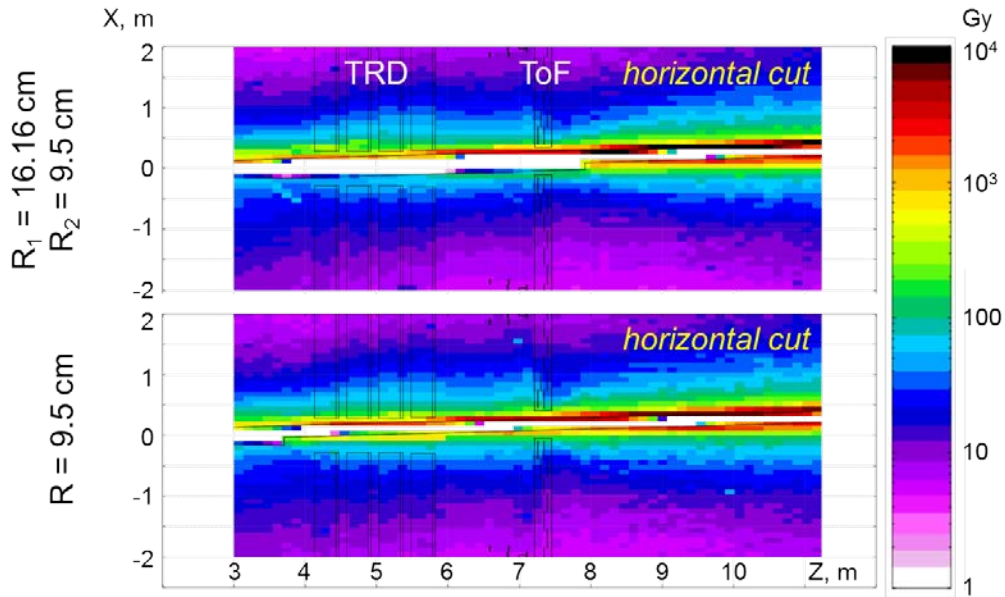


Fig.12: Ionizing dose in the CBM cave for the two beam pipe options (see text).

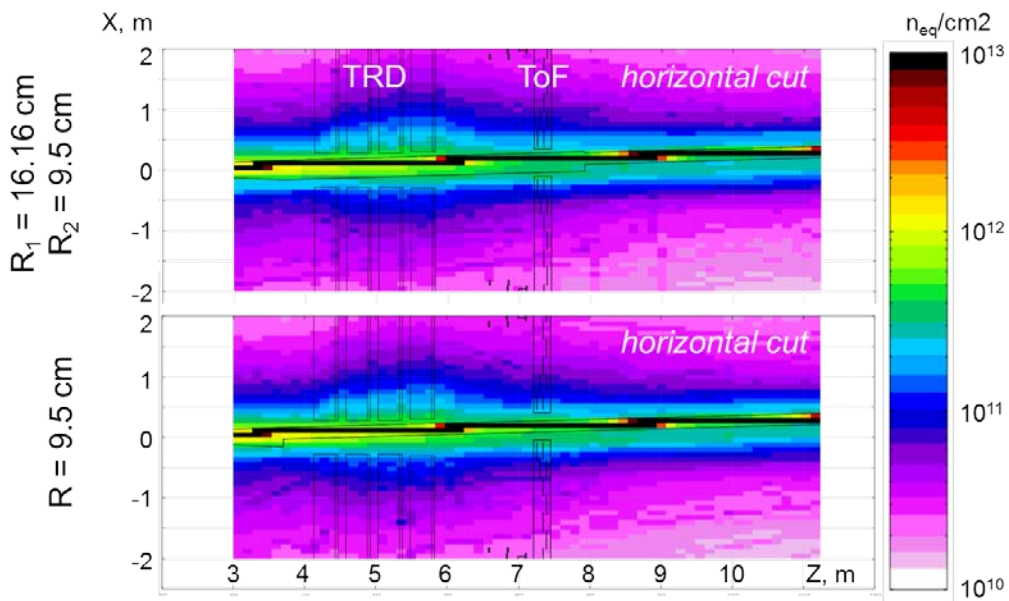


Fig.13: Non-ionizing dose in the CBM cave for the two beam pipe options (see text).

1.6 Next steps

Two options for the CBM beam pipe have been developed using FLUKA calculations. Both options share the section through the STS and RICH/MuCh, followed by the bellow which has to provide a tilt of the subsequent beam pipe section with angles between 0.7 and 1.8 degrees for Au beams depending on energy and magnetic field. The deflection angle should not exceed a value of 2.3 degrees, otherwise the beam will no longer hit the iron core of the beam dump which is located 26 m downstream the



This project has received funding from the European Union's Horizon 2020 research and innovation programme under grant agreement No. 871072.

target and has a lateral width of 2 m. For beams with lower Z/A than gold the magnetic field has to be lowered, or, if possible, a higher beam energy should be used.

Downstream the bellow two options are proposed. In one version, the beam pipe continues with a radius of $R = 16.16$ cm up to the entrance of the PSD, where the radius is reduced to $R = 9.5$ cm. This narrower beam pipe is horizontally displaced by 5 cm with respect to the wider one, in order to have the beam centered in the pipe. In the other version, the beam pipe with radius $R = 9.5$ cm starts already after the bellow, with a horizontal displacement of 6.5 cm.

According to the FLUKA calculations both beam line options show the same performance concerning the background radiation level in the detectors and in the cave. The next step is to use the beam pipe models for physics simulations, in order to study the influence of the additional background radiation on the performance of global track reconstruction and particle identification. Particularly important is the study of the performance of the PSD concerning event plane reconstruction which might suffer most from the additional radiation. In order to prepare these simulations, the two beam line options have been implemented into CBMroot. The models are shown in figure 14. In parallel to the simulations, an engineering design can be developed in order to work out the technical details like a pipe bending mechanism, support structures etc., which might create additional background to be included in the second round of simulations.

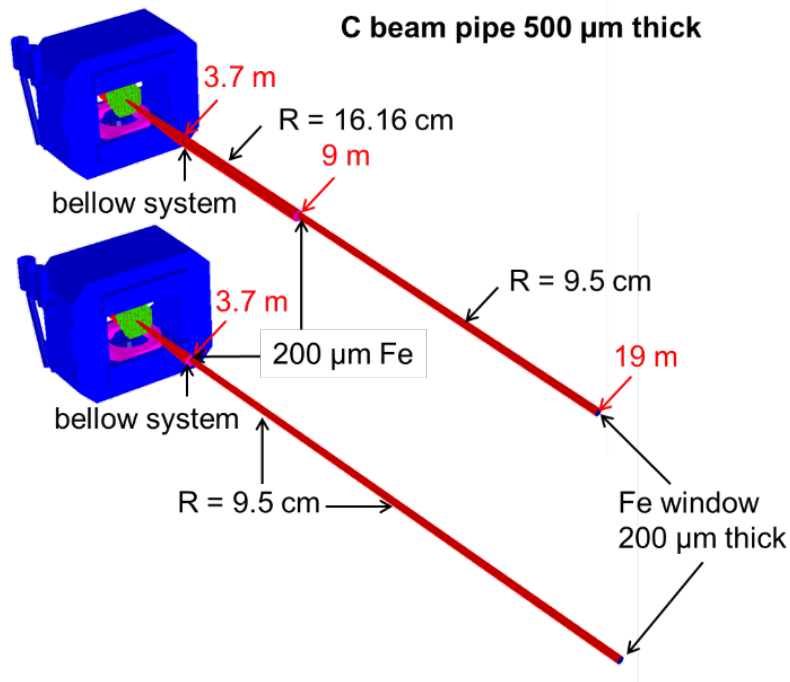


Fig. 14: Models of the two beam pipe versions in CBMroot.

2. Beam pipe and target chamber studies for the BM@N experiment at NICA



This project has received funding from the European Union's Horizon 2020 research and innovation programme under grant agreement No. 871072.

2.1 Radiation calculations without and with beam pipe downstream the target

A well focused Nuclotron beam together with an evacuated beam pipe downstream the target as will fulfil the experimental requirements for measuring Au+Au collisions at high beam intensities. In order to demonstrate the necessity of a beam pipe downstream the target, FLUKA calculations have been performed, assuming no beam pipe downstream the target, as it is the case in the present BM@N setup. The beams used so far go in air through the magnet and the detector areas. In the case of an Au beam with an energy of 5 A GeV, an intensity of $2 \cdot 10^6$ ions/s and an Au target of 250 μm thickness, such a situation would result in charged particle density rates in the detector areas as shown in figure 15. The rate densities reach values of up to 1 MHz/cm^2 , similar values have been discussed above for the present Nuclotron beam, where an evacuated beam pipe downstream the target has been assumed. Note, that the FLUKA calculations illustrated in figure 8 have been performed without a beam pipe downstream the target, but with a well-focused beam from the Nuclotron, assuming a rectangular shape of size $x = y = 0.6 \text{ mm}$ with a divergence of 1.7 mrad.

The high values for the electron rate densities shown in figure 8 clearly call for an improvement of the situation. As already discussed above, an evacuated beam pipe downstream the target would be the optimal solution. However, in order to investigate the possibility of a technically simpler option, FLUKA simulations have been performed for a beam pipe downstream the target, which is filled with Helium. The shape of the Helium filled beam pipe is shown in figure 16. The beam pipe is made of polyvinylfluoride of 30 μm thickness, and has a Beryllium foil of 250 μm thickness to separate the beam vacuum from the Helium. In the following, results of FLUKA calculations will be presented for an Au beam with an energy of 5A GeV, an intensity of $2 \cdot 10^6$ ions/s, a rectangular beam shape of size $x = y = 0.6 \text{ mm}$ with a divergence of 1.7 mrad at the target, and an Au target of 250 μm thickness.

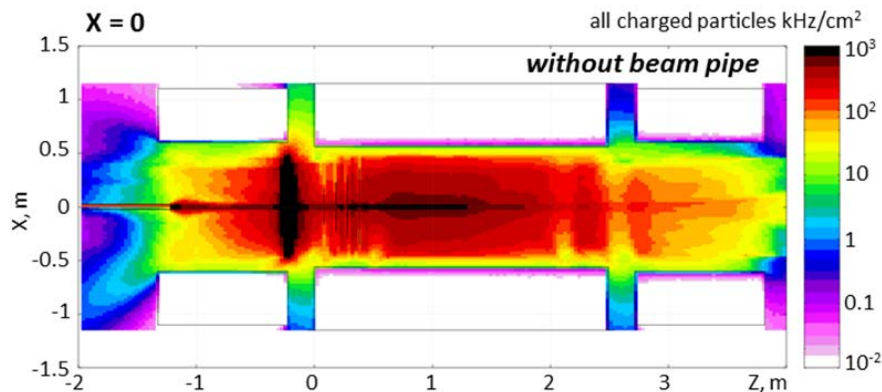


Fig. 15: Charged particle densities in the vertical plane along the beam inside the magnet with a well-focused beam from the Nuclotron, but without beam pipe downstream the target.



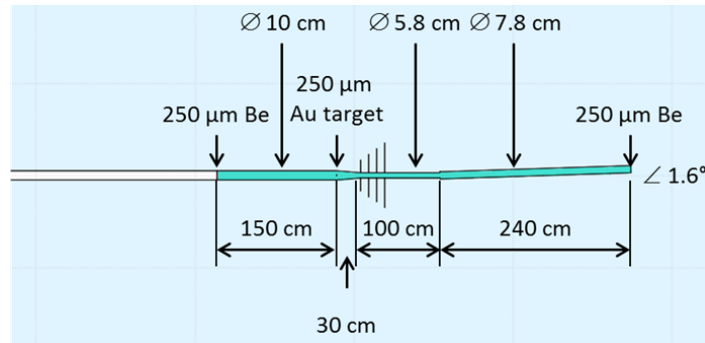


Fig. 16: Helium filled beam pipe made of 30 μm thick PVF foil, and with a 250 μm thick Be-window locate 150 cm upstream the target.

In figure 17 the rate density of charged particles (mainly delta electrons) in the silicon tracking stations is shown for the case of the Helium filled beam pipe (upper panel), and for the vacuum beam pipe (lower panel). In case of the Helium filled beam pipe, the delta electrons are produced in the Be-foil, in the target, and in the Helium. The resulting rate density reaches values of up to $10^5 \text{ cm}^{-2}\text{s}^{-1}$. In case of the vacuum beam pipe, the delta electrons are produced in the target and in the pipe material, and the rate densities go up to $5000 \text{ cm}^{-2}\text{s}^{-1}$. These values should be compared to the proton rate density in the silicon sensors shown in figure 18. Most of these protons are produced in minimum bias collisions of two Au nuclei in the target, and should be measured with high efficiency. In the central part of the silicon detector stations, the proton rate reaches values of about 2 kHz/cm^2 , which is a factor of about 2.5 lower than the charged particle rate densities calculated for the vacuum beam pipe, which include electrons, pions, and protons.

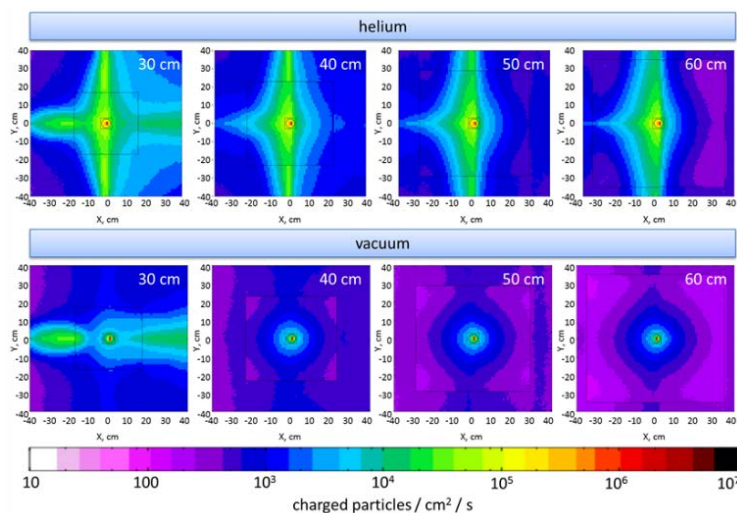


Fig. 17: Charged particle densities in the four STS stations for the Helium filled beam pipe (upper panel) and for the vacuum beam pipe (lower panel). The simulations have been performed for an Au beam with an intensity of $2 \cdot 10^6$ ions/s. The lower panel is identical to the lower panel in figure 2. Details see text.



This project has received funding from the European Union's Horizon 2020 research and innovation programme under grant agreement No. 871072.

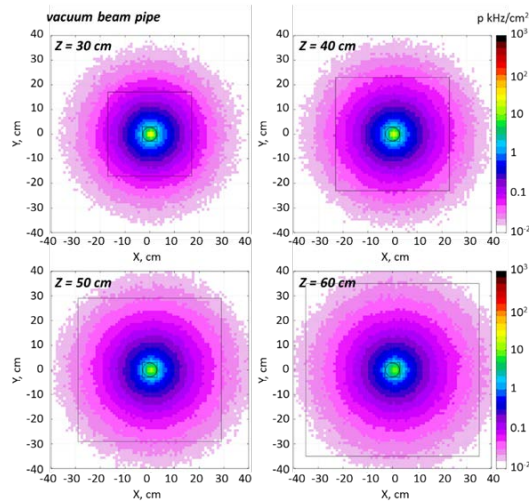


Fig. 18: Proton densities in the four STS stations calculated for the vacuum beam pipe. The values obtained for the Helium beam pipe are very similar, as most of these protons stem from minimum bias Au+Au collisions in the target. The simulations have been performed for an Au beam with an intensity of $2 \cdot 10^6$ ions/s.

The particle density rates at a distance of 2 m downstream the target, in a region where the GEM tracking stations are located, are shown in figure 19 both for the Helium beam pipe (upper panel) and for the vacuum beam pipe (lower panel). For the Helium beam pipe electron rates of up to $10^5 \text{ cm}^{-2}\text{s}^{-1}$ are reached.

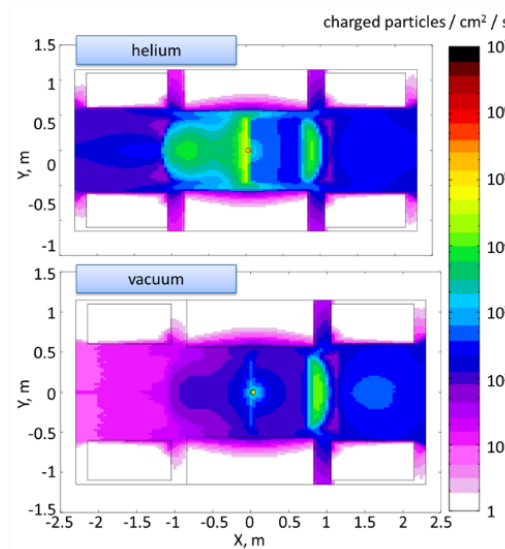


Fig. 19: Charged particle densities at a distance of 2 m downstream the target where the GEM tracking stations are located, for the Helium beam pipe (upper panel) and for vacuum beam pipe (lower panel). The simulations have been performed for an Au beam with an intensity of $2 \cdot 10^6$ ions/s. Details see text.



This project has received funding from the European Union’s Horizon 2020 research and innovation programme under grant agreement No. 871072.

FLUKA calculations have been performed to study the ionizing and non-ionizing dose. Figure 20 depicts the horizontal and vertical distributions the ionizing dose after two months of running for the Helium beam pipe (upper panel) and for the vacuum beam pipe (lower panel). In the first case the Silicon detector stations will be irradiated with an ionizing dose of 100 Gy in a vertical area of about 15 cm width (see upper right panel), whereas in the lower panel values of 5 – 10 Gy are reached. A dose of 100 Gy reached after 2 months already would correspond to a mild damage of a substantial part of the silicon sensors. The non-ionizing dose in the location of the silicon stations reaches values between 10^{10} and 10^{11} n_{eq}/cm^2 , a dose which will be tolerated by the sensors.

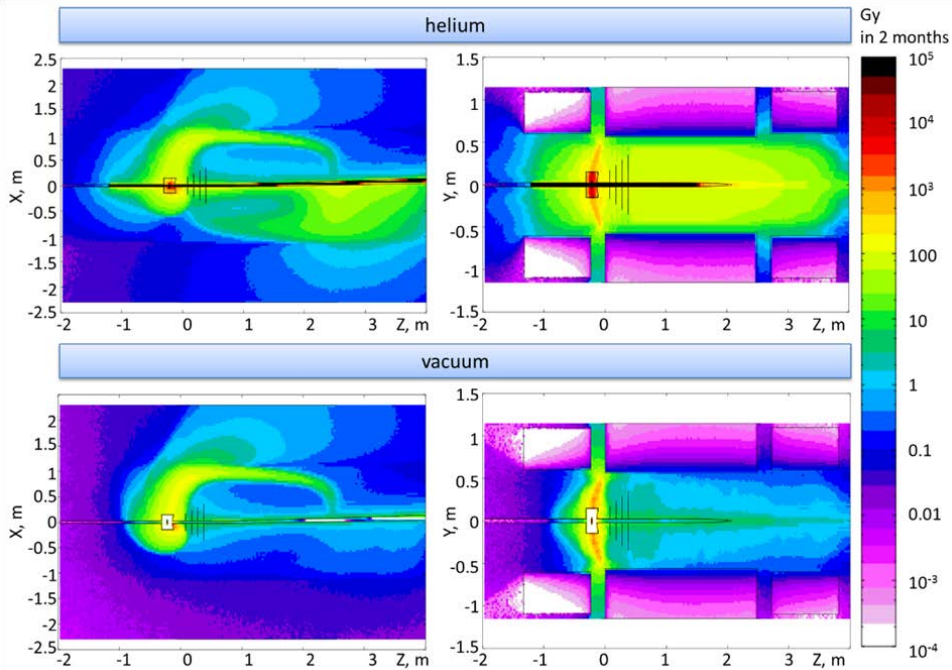


Fig. 20: Ionizing dose in Gray in the horizontal (left column) and vertical plane (right column along the beam in the BM@N experiment after two months of running with an Au beam of 5A GeV with an intensity of $2 \cdot 10^6$ ions/s. The upper row refers to the helium filled beam pipe, the lower row to the vacuum beam pipe.

The results of the simulations clearly demonstrate that the BM@N experiment has to be equipped with a vacuum beam pipe in order to protect the detectors from severe radiation damages.

References

- [1] The FLUKA code. G. Battistoni et al., Proceedings of the Hadronic Shower Simulation Workshop 2006, Fermilab, 6 – 8 Sept. 2006
- [2] Vasilisa Lenivenko, private communication
- [3] M. Kapishin, private communication

2.2 Preliminary design of the BM@N target chamber and beam pipe



This project has received funding from the European Union's Horizon 2020 research and innovation programme under grant agreement No. 871072.

The preliminary concept of the target chamber and the beam pipe is shown in figure 21. Both target chamber and pipe are made from carbon fiber material with a wall thickness of 1 mm. The idea of the design is, that the beam pipe exhibits a fixed curvature, according to the bending angle of a gold beam at the highest Nuclotron energy of 4.5 A GeV for a magnetic field of 0.9 T. For beams with lower energies, the magnetic field will be reduced such, that the beam fits into the pipe. The upper panel of figure 21 depicts the target chamber and the first inclined part of the beam pipe, whereas the lower panel illustrates the rest of the beam pipe with three more kinks.

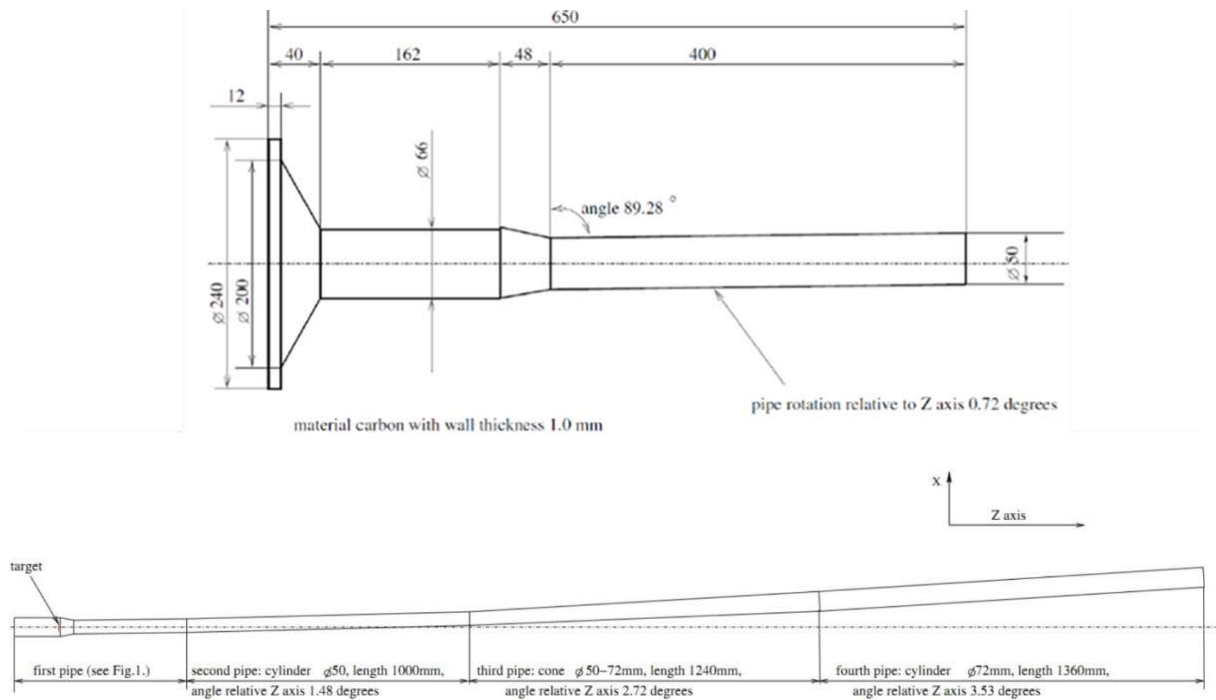


Fig. 21: Upper panel: Design of the target chamber together with the first part of the beam pipe of the BM@N experiment, made of 1 mm thick carbon fiber material. Lower panel: Sketch of the curved beam pipe of the BM@N experiment from target to beam dump.

The beam pipe consists of four straight parts separated by the kinks, as illustrated in lower panel in figure 21. These parts will be connected by a special coupling pipe without flanges in order to reduce the material budget. A preliminary engineering design of a beam pipe connection with a kink is shown in figure 22. The coupling and the kink is performed by a tube of 100 mm length and about 3 mm wall thickness, and the vacuum tightness is provided by four Viton O-rings. Figure 23 depicts photos of the first prototype beam pipe pieces.



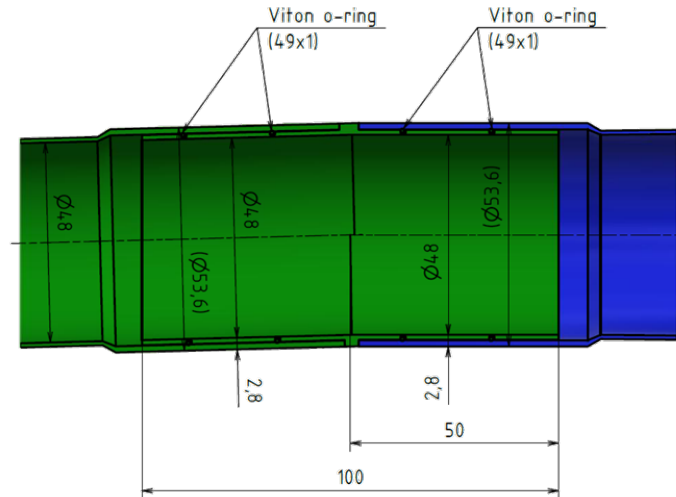


Fig. 22: Preliminary engineering design of a flangeless beam pipe connection with a kink angle. Vacuum tightness is provided by four Viton O-rings.



Fig 23: Photos of prototype beam pipe pieces from carbon fiber material.

3. Design of beam monitors for the CBM experiment at FAIR

3.1 Introduction

The aim of this project is to develop and deliver a high-speed time-zero (TO) detector on chemical vapour deposition (CVD) diamond basis. This detector must meet the requirements of the time-of-flight (ToF) measurement system for beams of protons and heavy ions. The system should have a time resolution of better than 50 ps (sigma) and stable long-term detector operation at high interaction rates of 10^7 particles/s with a detection efficiency of almost 100%. The beam detectors will be integrated inside the CBM beamline as shown in Fig. 24.

To achieve these goals, a fast detector is used in combination with fast readout electronics. At the same time, the detector could be used for the online beam monitoring and information on the beam profile and stability of the beam can be obtained, i.e. its position on the target, the amount of halo particles and the time structure of the beam.



This project has received funding from the European Union's Horizon 2020 research and innovation programme under grant agreement No. 871072.

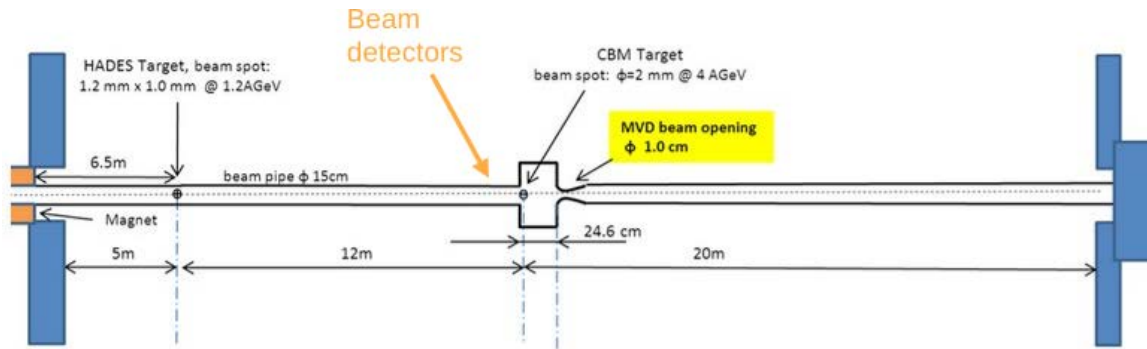


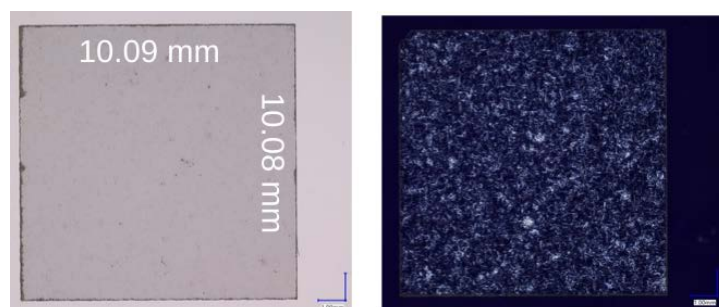
Figure 24: CBM beamline geometry. Taken from [1].

3.2 Concept of diamond based T0 detector for Day-1

Experiments with high-intensity heavy ion beams require fast and radiation-hard detection systems. For these purposes, pcCVD and scCVD diamond detectors (poly- and single-crystal CVD materials) are widely used. Its Radiation hardness and excellent timing characteristics make the diamond material an almost ideal choice for our application. In the proposed concept we plan to develop the time-zero start detector utilizing the commercially available electronic grade CVD diamond material produced by Element Six [2].

In physics production experiments with heavy ions, it could be shown [3] that a CVD diamond-based time-zero-start detector fulfilled the requirements in terms of time resolution and radiation hardness. The proposed CBM T0 sensor will be equipped with double-sided strip metallization with perpendicular strip orientation. Assuming the strip pitch of about 100 μm and the beam size of about 1 cm diameter we expect to be able to measure up to 10^8 particles/s keeping the particle rate per channel below of 10^6 ions/(s*channel), which is a moderate rate for the available read-out system.

In the preparation phase a set of the CVD diamond sensors is planned to be produced. Several pieces of CVD diamond material produced by Element Six have been ordered, sliced and polished, obtaining the final thickness of about 80 μm . The sensor thickness has to be kept below 100 μm to minimize the beam interaction probability in the sensor material and reduce the background events. The machined diamond plates for sensors have been optically inspected at the GSI Detector Laboratory showing excellent surface quality, an example pictures are shown in Fig. 25.



This project has received funding from the European Union's Horizon 2020 research and innovation programme under grant agreement No. 871072.

Figure 25: Optical inspection of CVD sensors. Picture by Michael Träger (GSI, Detector Laboratory).

In Q2 2021 we plan to develop and establish the final geometry of the strips. It is necessary to correctly estimate the capacitance of the selected strip geometries in order to minimize the capacitive coupling between neighboring strips and between two sides of the detector. The strip metallization will be performed at the GSI Detector Laboratory.

The sensor will be mounted on a dedicated printed circuit board (PCB) equipped with amplifier and shaping circuits. This board is connected to two additional PCBs, used as feedthrough to transport the analog signals outside the vacuum. A sketch of such PCBs is shown in Fig. 26 (left). The system will be mounted in the CBM beamline, inside of a cubic vacuum chamber, as shown in Fig. 26 (right).

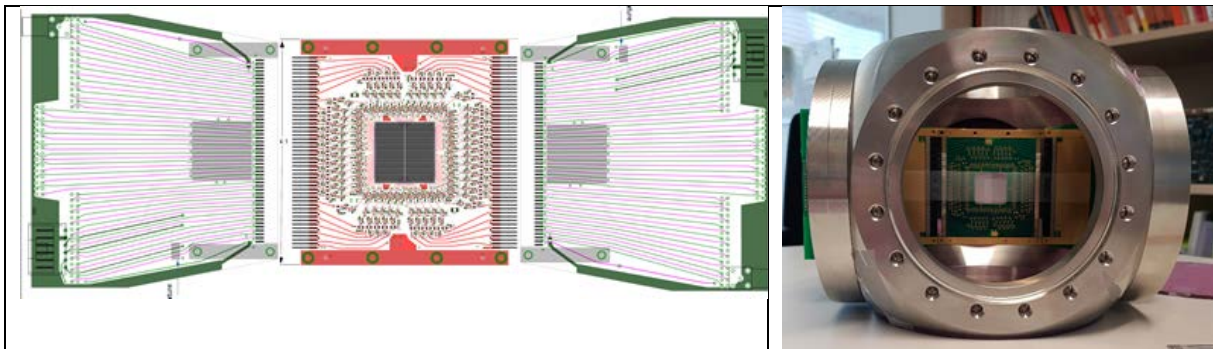


Figure 26: Left: Modular read-out board with the diamond sensor mounted in its center. Design by W. Koenig, GSI Right: The beam detector will be mounted in the CBM beamline inside a cubic vacuum chamber.

3.3 Beam halo measurement concept

To ensure the stable operation of the CBM detector, it is necessary to minimize the amount of halo particles entering the detection system. For this purpose a dedicated beam collimation system is foreseen at the SIS100 accelerator complex. The CBM detector has to be equipped with a system capable of precisely measuring beam halo particles.

The precise measurement must be based on the time of arrival of the individual particles. Additionally, a Time over Threshold (ToT) measurement is necessary, which will be used to monitor the efficiency and radiation damage of the system. For the beam halo measurement we plan to construct a detector by means of four active sensors positioned about 0.5cm from the beam axis. The concept is shown in Fig. 27. Such an arrangement will allow us to monitor the position of the beam during the extraction process. The results of the measurement will be used for securing the detectors, mainly the Micro Vertex Detector (MVD) and the Silicon Tracking System (STS) against sudden changes in the position of the beam. Besides this, it is planned to have a direct connection of the beam halo detector to a beam abort system.



This project has received funding from the European Union's Horizon 2020 research and innovation programme under grant agreement No. 871072.

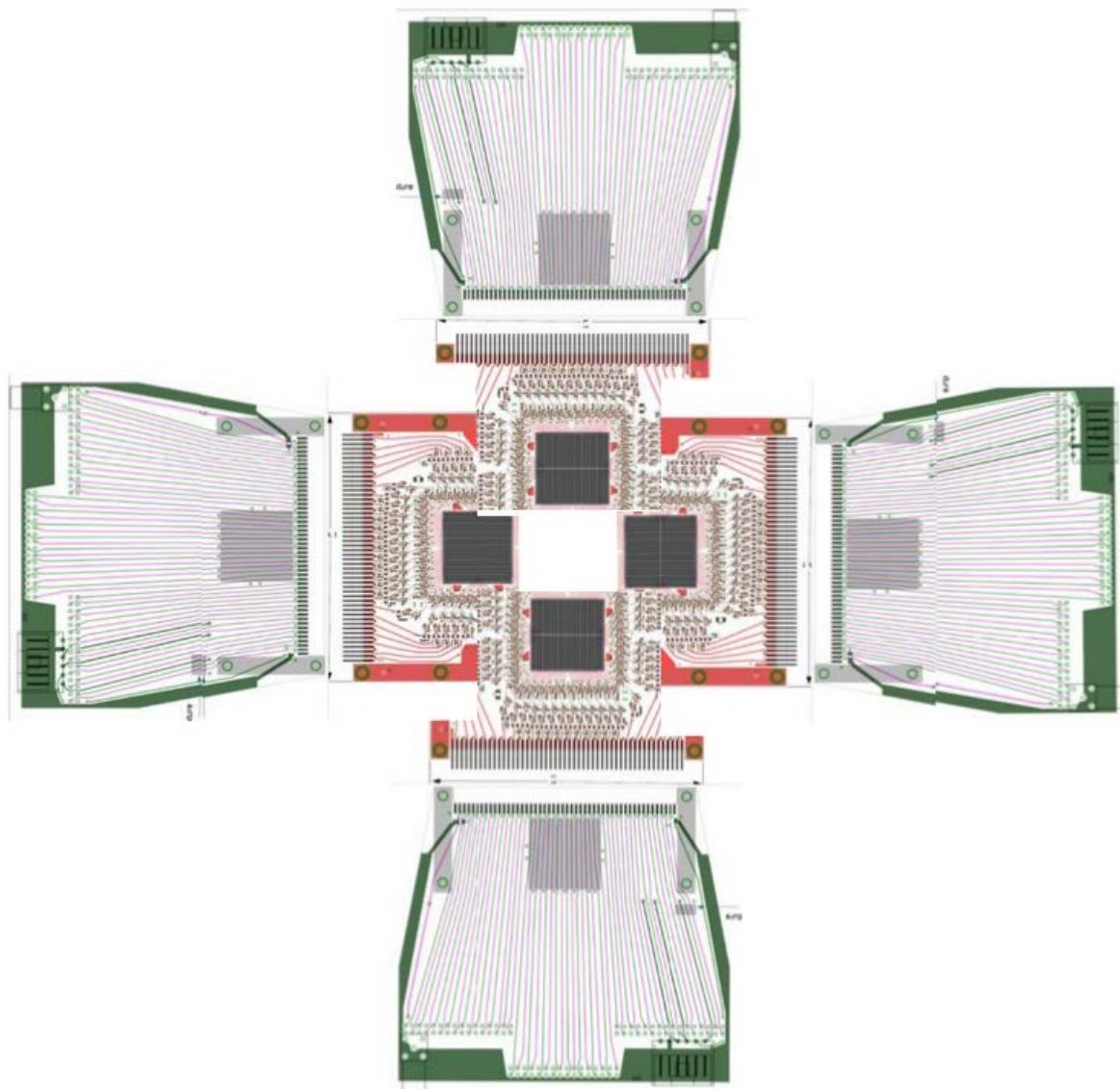


Figure 27: Beam halo measurement system by means of four active sensors positioned about 0.5 cm from the beam axis.

3.4 Mechanical integration

The CBM beam detector system will consist of two detector stations. One will be used for the beam HALO and the second one for the T0 measurement. Both detectors will be mounted inside a beampipe as schematically shown in Fig. 28. We propose to use commercially available vacuum elements and integrate them into the CBM beamline in front of the reaction target.



This project has received funding from the European Union's Horizon 2020 research and innovation programme under grant agreement No. 871072.

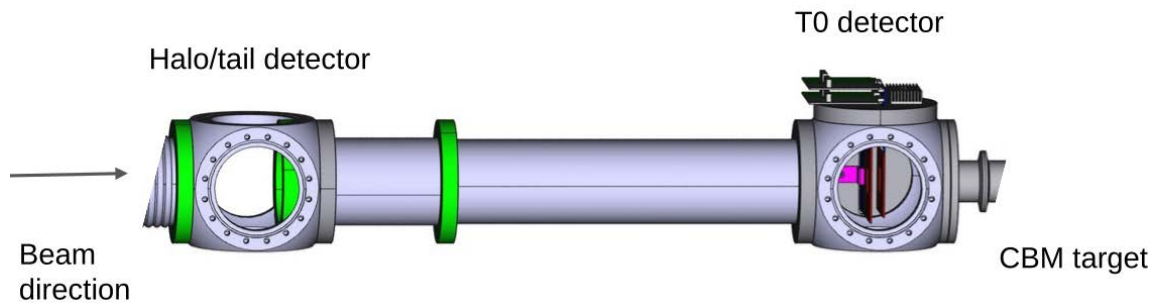


Figure 28: Beampipe with two stations of beam detectors which will be used for beam HALO and T0 measurement.

3.5 Read-out concept

The concept of the read-out system is currently being developed and its evaluation is based on the experiences of the HADES T0 detector. It takes into account the currently being developed readout chains of the CBM experiment, mainly TOF and Ring Imaging Cherenkov (RICH) detectors. The HADES collaboration has been using similar detectors for in-beam measurements and recently demonstrated excellent online monitoring capabilities of the system based on diamond sensors and TRB readout system [4].

The read-out concept for CBM is schematically shown in Fig. 29. The sensor signals are amplified on a Front End Electronics (FEE) and afterwards sent to dedicated discriminator boards. Then a fan-out of the signals will be applied. One branch will deliver the T0 measurement for the CBMs read-out electronics using either CBM TOF TDC system or the TRB based time-to-digital converter (TDC) system as proposed in CBM RICH detector. The second branch of the beam detectors readout, independent from the CBM DAQ system, will be used for an "online" beam monitoring purposes and for the fast beam abort system.

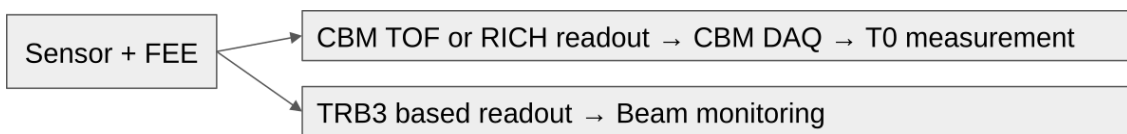


Figure 29: Read-out concept of the beam sensors. The T0 measurement has to be integrated into the standard CBM DAQ. A signal splitting will ensure a CBM-DAQ independent beam-monitoring.

3.6 Summary and outlook

The design of beam monitors and T0-counters for CBM have been shown. We are currently developing a sensor system based on CVD diamond technology. The system will be used for T0 measurement and beam monitoring purposes i.e. a beam halo particle measurement. Diamond sensors have been prepared. Next steps are to develop and establish the final geometry of the strips.



Currently the HADES collaboration is evaluating a new detector technology based on Low Gain Avalanche Detectors (LGAD). First beam test showed promising results to use this technology for in-beam detectors [5]. In parallel to the development of CVD diamond based sensors we will also evaluate this technology to use it in the CBM experiment.

Acknowledgements

We would like to thank TU Darmstadt and GSI Detector Laboratory for the preparation of the diamond sensors.

References

- [1] The CBM collaboration: Technical Design Report for the CBM Time-of-Flight System (TOF) (2014)
- [2] Element Six: <https://e6cvd.com/>
- [3] J. Pietraszko, T. Galatyuk, V. Grilj, W. Koenig, S. Spataro, and M. Träger, “Radiation damage in single crystal CVD diamond material investigated with a high current relativistic ^{197}Au beam,” Nucl. Instrum. Meth., vol. A763, pp. 1–5, 2014.
- [4] A. Rost, J. Adamczewski-Musch, T. Galatyuk, S. Linev, J. Pietraszko, M. Sapinski, and M. Traxler, “Performance of the CVD Diamond Based Beam Quality Monitoring System in the HADES Experiment at GSI*,” in Proceedings, 10th International Particle Accelerator Conference (IPAC2019): Melbourne, Australia, May 19-24, 2019.
- [5] Pietraszko, J., Galatyuk, T., Kedych, V. et al. Low Gain Avalanche Detectors for the HADES reaction time (T0) detector upgrade. Eur. Phys. J. A 56, 183 (2020).

